

## A FAR-FIELD RADIATION PATTERN MEASUREMENT METHOD FOR ELIMINATING RESIDUAL REFLECTIONS BY DISTANCE CHANGING

Kazushi NISHIZAWA, Yoshihiko KONISHI, Isamu CHIBA and Takashi KATAGI

Mitsubishi Electric Corporation

5-1-1, Ofuna, Kamakura-shi, Kanagawa 247, Japan

### 1. Introduction

For antenna radiation pattern measurements, residual reflections caused by a measurement environment should be suppressed as far as possible in order to evaluate accurate antenna radiation characteristics [1], [2]. For example, low-sidelobe antennas such as satellite antennas with sidelobe level less than -30dB have to be measured in low reflection condition. Usually, residual reflections are minimized by measuring a height pattern and by placing microwave absorbers on reflection points [3]. However, this cannot separate and eliminate measurement errors due to residual reflections from the measured radiation pattern. Several methods have been investigated for eliminating reflections [4], [5].

In this paper, authors propose a modified far-field antenna radiation pattern measurement method for eliminating residual reflections by using a range distance changing and the Fourier transformation. It is confirmed by a pattern measurement of an L-band standard gain horn that this method is effective to eliminate reflections.

### 2. Theory

Figure 1 shows a radiation pattern measurement model with a reflected wave #  $i$  caused by a side wall. In this figure, a direct wave and  $N$  reflected waves exist between a transmitting antenna (Tx antenna) and an antenna under test (AUT).  $r_0$  is a range distance between the Tx antenna and the AUT.  $r_{i1}$  and  $r_{i2}$  mean propagation distance for the reflected wave #  $i$  between the Tx antenna and the side wall and between the side wall and the AUT. The electric field  $E[\theta_{r_0}, r_0]$  received by the AUT is given by:

$$E[\theta_{r_0}, r_0] = E_t[\theta_{t_0}] \cdot E_r[\theta_{r_0}] \frac{e^{-jk_0 r_0}}{r_0} + \sum_{i=1}^N a_i \cdot E_t[\theta_{t_i}] \cdot E_r[\theta_{r_i}] \frac{e^{-jk_0 r_{i1}}}{r_{i1}} \frac{e^{-jk_0 r_{i2}}}{r_{i2}} \quad (1)$$

where  $E_t$  and  $E_r$  are electric radiation patterns of the Tx antenna and the AUT, respectively.  $\theta_{t_0}$  and  $\theta_{r_0}$  are a transmit angle of the Tx antenna and a receive angle of the AUT for the direct wave.  $\theta_{t_i}$  and  $\theta_{r_i}$  are those for the reflected wave #  $i$ .  $a_i$  is a reflection coefficient of the side wall.  $k_0$  is the wave number in the free space for measured frequency  $f_0$ . Fig. 2 shows an example of received electric fields  $E[\theta_{r_0}, r_0]$  at angles  $\theta_{r_0} = 0 - 60^\circ$  versus the range distance  $r_0$ . When  $r_0$  increases, the electric fields decrease accompanied by fluctuations. Next, the function  $F$  is determined as follows:

$$F[\theta_{r_0}, r_0] = E[\theta_{r_0}, r_0] \frac{r_0}{e^{-jk_0 r_0}} = E_t[\theta_{t_0}] \cdot E_r[\theta_{r_0}] + \sum_{i=1}^N a_i \frac{r_0}{r_{i1} \cdot r_{i2}} E_t[\theta_{t_i}] \cdot E_r[\theta_{r_i}] \cdot e^{-jk_0 \Delta_i} \quad (2)$$

where  $\Delta_i = r_{i1} + r_{i2} - r_0$ .  $F$  consists of the first d-c term for the direct wave and the second fluctuated terms for the reflected waves. Figure 3 shows an example of the amplitude of  $F$  calculated from Fig. 2. As shown in Fig. 3, the d-c term is superimposed by the fluctuated term at each  $\theta_{r_0}$ . Therefore, the d-c term and the fluctuated terms can be separated from each other by using the Fourier transformation with respect to  $r_0$ . Then, the Fourier spectrum  $G[\theta_{r_0}, f_r]$  is given for  $F[\theta_{r_0}, r_0]$  as follows:

$$G[\theta_{r_0}, f_r] = \frac{1}{R_2 - R_1} \int_{R_1}^{R_2} F[\theta_{r_0}, r_0] \cdot e^{j k_r r_0} dr_0$$

$$= E_t[\theta_{r_0}] \cdot E_r[\theta_{r_0}] \cdot e^{j \frac{R_2 - R_1}{2} k_r} \frac{\sin u_0}{u_0} + \frac{1}{R_2 - R_1} \sum_{i=1}^N \left\{ \int_{R_1}^{R_2} a_i \frac{r_0}{r_{i1} \cdot r_{i2}} E_t[\theta_{r_0}] \cdot E_r[\theta_{r_0}] \cdot e^{j(k_r r_0 - k_{i1} r_{i1} - k_{i2} r_{i2})} dr_0 \right\} \quad (3)$$

$$u_0 = \frac{R_2 - R_1}{2} k_r, \quad k_r = \frac{2\pi}{c} f_r \quad (4)$$

where  $f_r$  is fluctuating frequency for  $F$ ,  $k_r$  is wave number of  $f_r$ , and  $c$  is velocity of light.  $R_1$  and  $R_2$  are the minimum and maximum of  $r_0$ , respectively.

When a difference of the range distance  $R_2 - R_1$  is much larger than the summation in the second term of Eq. (3), the Fourier spectrum  $G$  becomes as follows for  $f_r = 0$ :

$$G[\theta_{r_0}, f_r = 0] \approx E_t[\theta_{r_0}] \cdot E_r[\theta_{r_0}]. \quad (5)$$

Equation (5) expresses the d-c term for the direct wave in Eq. (2), that is, the accurate electric radiation pattern of the AUT  $E_r[\theta_{r_0}]$ , because  $E_t[\theta_{r_0}]$  is a constant value.

### 3. Experiment

We performed a far-field radiation pattern measurement for an L-band standard gain horn antenna in order to evaluate the proposed method. Measurement parameters are shown in Table 1. Radiation patterns at each  $r_0$  are measured in two different reflection conditions : without/with microwave absorbers on the floor of the anechoic chamber. Figure 4 shows far-field radiation patterns at each  $r_0$  without microwave absorbers. The shape of the measured radiation patterns varies noticeably for  $r_0$  because of a large reflection from the floor. Figure 5 and Figure 6 show the respective Fourier spectrums  $G$  at  $\theta_{r_0} = 0^\circ$  without/with microwave absorbers. Solid lines denote the spectrums  $G$  obtained from the measured radiation patterns and dashed lines show the expected spectrums when no reflection exists (the first term of Eq. (3),  $\sin u_0 / u_0$ ). As shown in Fig. 5, the obtained spectrum  $G$  for the measured patterns is quite different from the expected one at  $f_r = -0.3\text{GHz}$ . However, the obtained spectrum in Fig. 6 is similar to the expected one. The Fourier spectrum for the reflected wave from the floor is observed at  $f_r \approx -0.3\text{GHz}$ . Figure 7 shows an accurate amplitude and phase radiation patterns for the direct wave calculated by Eq. (5) in the two different reflection conditions. These two patterns are in good agreement. The difference of amplitude patterns is less than -54dB and the difference of phase patterns is less than  $10^\circ$  for the amplitude pattern >-40dB. Thus, the proposed method is effective in order to eliminate residual reflections.

### 4. Conclusion

Authors proposed a modified far-field antenna radiation pattern measurement method in order to eliminate residual reflections by changing a range distance. It was confirmed that residual reflections could be suppressed to about -50dB by the pattern measurement at L-band. The proposed method is effective for evaluating accurate radiation patterns.

### References

- [1] IEICE, *Antenna Engineering Handbook*, pp. 427-439 (1980) (in Japanese).
- [2] W. F. Kummer and F. S. Gillespie, "Antenna measurements-1978," *Proc. IEEE*, vol. 66, no. 4, pp. 427-439 (April 1978).
- [3] J. D. Kraus, *Antennas - Second Edition-*, McGraw-Hill, pp.811-813 (1988).
- [4] G. E. Evans, *Antenna Measurement Techniques*, Artech House, Chapter 4 (1990).
- [5] J. van Norel and V. J. Vokura, "Novel APC-methods for accurate pattern determination," *AMTA Proceedings*, pp. 385-389 (1993).

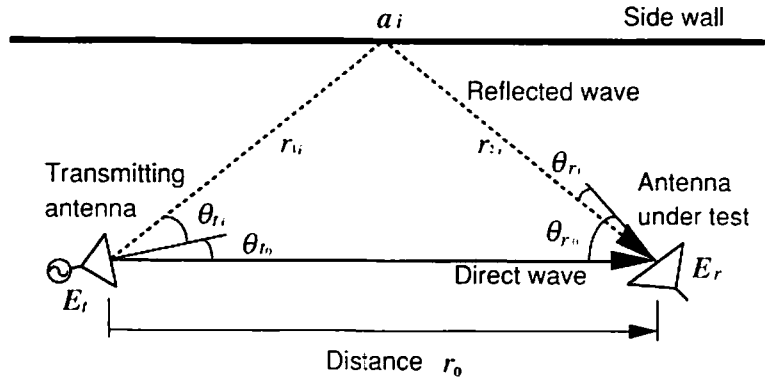


Fig.1 Radiation pattern measurement model with side wall reflections.

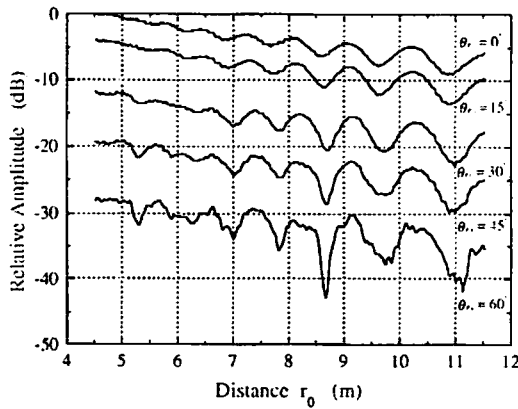


Fig.2 Amplitude vs. distance  $r_0$  for measured electric field  $E$ .

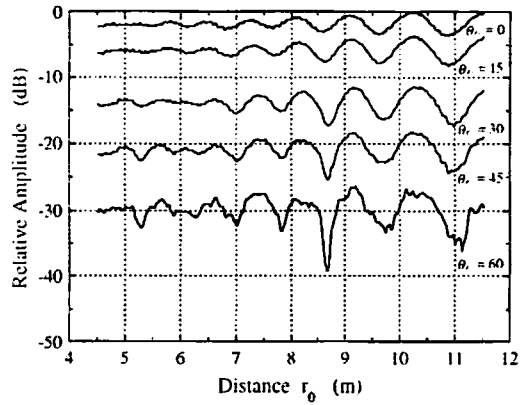


Fig.3 Amplitude vs. distance  $r_0$  for function  $F$ .

Table 1 Parameters used for the radiation pattern experiment.

Antenna under test	L-band standard gain horn antenna
Transmitting antenna	Ridged horn antenna
Polarization	Vertical polarization
Frequency	1.5GHz
Range distance	$R_1 \leq r_0 \leq R_2$ ; $R_1 = 4.525\text{m}$ , $R_2 = 11.525\text{m}$ ( $R_2 - R_1 = 7.0\text{m}$ )
Distance interval	25.0mm
Number of range distances	281
Surrounding condition	With and without microwave absorbers on the floor of the anechoic chamber

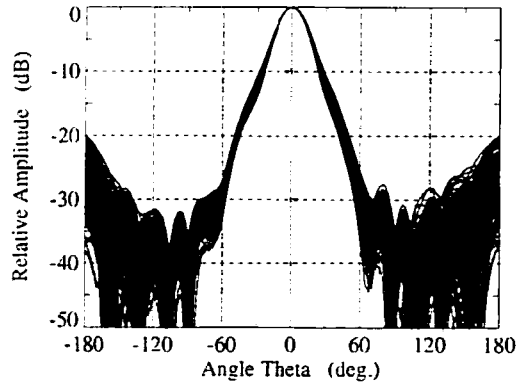


Fig.4 Measured radiation patterns in case of no absorbers existing on the floor.

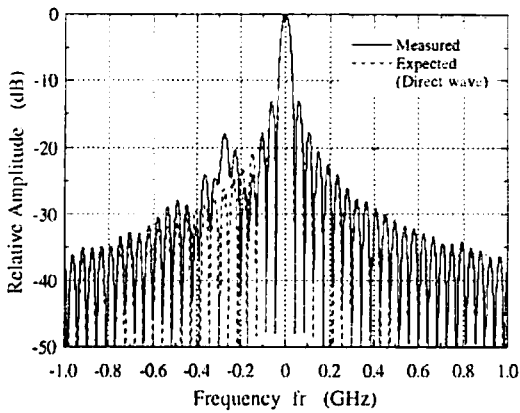


Fig.5 Fourier spectrum at  $\theta_{ra} = 0^\circ$  in case of no absorbers existing on the floor.

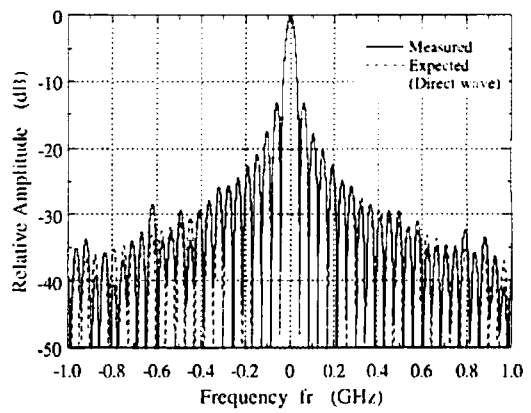
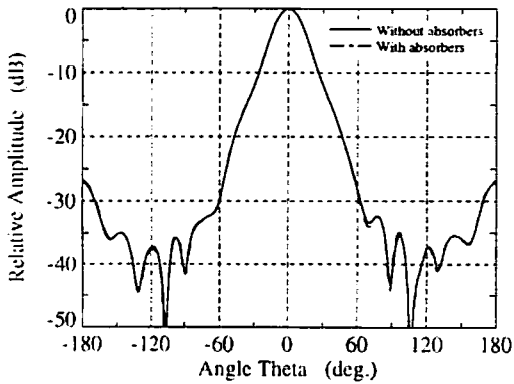
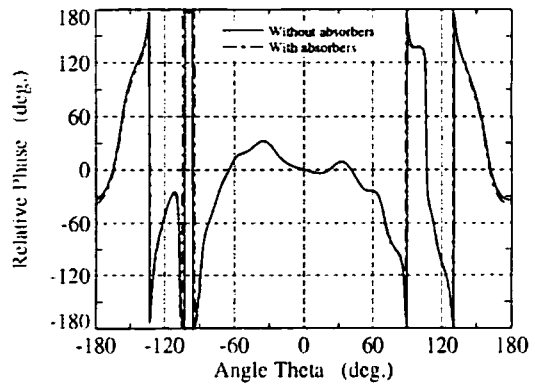


Fig.6 Fourier spectrum at  $\theta_{ra} = 0^\circ$  in case of absorbers existing on the floor.



(a) Amplitude



(b) Phase

Fig.7 Obtained radiation patterns in the two different reflection conditions.